Heterogeneous nucleation effects of talc particles on polymorphic crystallization of cocoa butter

Laura Bayés-García[a], Shinichi Yoshikawa[b], Mercedes Aguilar-Jiménez[a], Chinami Ishibashi[c,†], Satoru Ueno[c], Teresa Calvet[a]

[a]Departament de Mineralogia, Petrologia i Geologia Aplicada, Facultat de Ciències de la Terra, Universitat de Barcelona, Martí i Franquès, s/n, 08028, Barcelona, Spain

[b]Research Institute for Creating the Future, Fuji Oil Holdings INC., Osaka, Japan.

[c]Faculty of Applied Biological Science, Hiroshima University, Higashi-Hiroshima, Japan.

KEYWORDS: Polymorphism, crystallization, heterogeneous nucleation, additive, cocoa butter, talc, synchrotron radiation X-ray diffraction, DSC

ABSTRACT

Polymorphic crystallization of cocoa butter (CB) in a bulk system was examined for the influence of adding talc particles at different concentrations (0.1%–5%). While the system was cooled from the melt and subsequently heated, changes in the heat flow and crystal structure of CB were analyzed using differential scanning calorimetry (DSC) and synchrotron radiation X-ray

diffraction (SR-XRD). Synchrotron radiation microbeam X-ray diffraction (SR-μ-XRD) was employed to determine lamellar-plane directions of CB crystals occurring with talc addition. At any cooling rates (0.1–15 °C/min) applied, talc promoted CB crystallization to elevate the onset crystallization temperature logarithmically with the increasing concentration of talc; this effect became more prominent at higher cooling rates. Talc also acted as a polymorphic stabilizer, so that CB crystallized in more stable forms even when cooled at the highest rate of 15 °C/min. Moreover, a highly ordered lamellar-plane direction was extensively observed for CB crystals occurring with 0.1% talc addition, which was disturbed by 0.5% talc addition probably due to the spatial dispersion of densely populated talc particles in their randomized orientation. These heterogeneous nucleation effects indicate the potential of talc particles to be used for quality and productivity control of CB-based products.

INTRODUCTION

Cocoa butter (CB) is a pale-yellow edible fat with multiple usage in food, cosmetic and pharmaceutical industries.[1] When crystallized in chocolate products, CB constitutes the main body in which sugar crystals, cocoa particles and other ingredients are embedded. Being composed by three main triacylglycerols (TAGs) 1(3)-palmitoyl-2-oleoyl-3(1)-stearoyl-glycerol (POS), 1,3-distearoyl-2-oleoyl-glycerol (SOS), and 1,3-dipalmitoyl-2-oleoyl-glycerol (POP), CB presents unique crystal polymorphism responsible for the excellent sensory properties of sharp melting and quick flavor release provided by chocolate.[2] Among the six polymorphs Forms I–VI of CB crystals, Form V is intentionally developed in chocolate products through the tempering process to achieve desirable texture and mouthfeel.

Many researchers have investigated the polymorphic crystallization and transformation mechanisms of CB under isothermal and non-isothermal conditions, not only in bulk state,[3-6] but also under the effects of certain selected additives.[7,8] As an example, Loisel et al.[7] evaluated the influence of replacing CB partly with its indigenous minor components of tristearoylglycerol (SSS), distearoylglycerol, and stearic acid on chocolate crystallization and determined that incorporation of distearoylglycerol and stearic acid delayed the formation of SSS crystals and decreased their growth rate to a slight extent. Likewise, very recent work reported on the effectiveness of the addition of phospholipids at a concentration of the order of 0.1% on the crystallization of CB and commercial chocolate.[9] However, additives have been mostly employed in chocolate products to retard the occurrence of CB Form-VI crystals, a cause of fat blooming that deteriorates the product quality.[10-17] For this purpose, some of the additives employed have been fatty acid esters, acylglycerols, glycerolglycolipids, lipid (e.g. milk fat) fractions, or emulsifiers, among others.

Smith et al.[18] exhaustively reviewed effects of minor components in lipid systems on microscale fat crystallization and macroscale physical properties. In this review, it is stated that concentrations below 0.1% may be enough for the minor components to act as fat-nucleation modifiers, whereas higher concentrations between 0.5% and 5% are likely required for the ones to be incorporated in fat crystal structure. Since most of the minor components described are hydrophobic, more significant effects are expected when the chemical structure of acyl groups is similar between the minor components and fats crystallizing in the lipid systems. Additional work done by Mahisanunt et al.[19] have indicated the significance of polymorphic matching between TAG seed crystals and fat crystals occurring in lipid systems for the efficient fat crystallization, as observed that nucleation of coconut oil in the β′ polymorph was strongly

induced by seed crystals of tripalmitoylglycerol (PPP) or SSS in the same polymorph through epitaxial growth.

Yoshikawa and co-workers newly found the remarkable potential of inorganic compounds including talc as fat-crystallization promoters in lipid systems, despite their chemical structure lacking acyl groups.[20-22] Talc promoted crystallization of a mixed-acid monounsaturated TAG of POP as well as monoacid trisaturated TAGs of trilauroylglycerol (LLL), trimyristoylglycerol (MMM), and PPP in each isolated single TAG system. Talc also promoted crystallization of multi-component palm oil, elevating an initial crystallization temperature of the high-melting fraction represented by PPP and POP; consequently, adding talc particles to palm oil-based shortening improved the physical properties of viscoelasticity and hardness. Results on the isolated single TAG system of LLL have indicated that talc particles with median sizes below 2.5 μm and at concentrations above 0.1% effectively promote fat crystallization in more stable polymorphs and that this effect can be controlled by tuning the cooling rate applied. By analyzing the relative intensity between small- and wide-angle XRD peaks, different models were proposed for the adsorption of TAG molecules on both talc and graphite surfaces.[20] Very recent work,[23] using polarized Fourier-transform infrared spectroscopy combined with the attenuated total reflection sampling method, has offered the revised model that LLL molecules adsorb on graphite surfaces to make double-chain length layers parallel to the surfaces.

In the present work, we report on the heterogeneous nucleation effects of talc particles on polymorphic crystallization of multi-component CB in a bulk system and the dependency on concentrations of talc and crystallization conditions, using measurement techniques of differential scanning calorimetry (DSC) and synchrotron radiation X-ray diffraction (SR-XRD). Synchrotron radiation microbeam X-ray diffraction (SR-μ-XRD) was also employed to

determine lamellar-plane directions of CB crystals occurring with talc addition, which could be a clue for elucidating the adsorption mode of TAG molecules on talc surfaces. SR-μ-XRD has been applied to lipid systems, such as spherulites of LLL[24] and those of binary mixtures of POP/1,3-dipalmitoylglycerol (OPO),[25] palm oil,[26] water-in-oil emulsion,[27-29] and granular crystals occurring in palm-oil-based water-in-oil emulsion.[30]

Regarding the practical use of talc as an additive in CB products, we must note that (1) CB is widely employed not only in chocolate, but also in pharmaceuticals (e.g. suppository) or cosmetics (e.g. oily cream, where controlling the crystallization behavior is very important); and (2) talc is widely approved as pharmaceutical excipient and as a food-grade additive. According to EU regulations, talc is approved in some food products like sausages or rice, but it is still not listed for CB and chocolate products. The present work becomes a fundamental research for which we analyzed the effects of talc as an inorganic additive to a complex lipid system having complex polymorphic behavior, which is CB.

EXPERIMENTAL SECTION

Materials

CB was donated by Simon Coll Xocolaters S.A. (Sant Sadurní d'Anoia, Spain).

A talc powder sample NANO ACE D-600, consisting of particles having a median size of 0.6 μm, was purchased from Nippon Talc (Osaka, Japan). Talc particles were added to CB at weight fractions of 0.1%, 0.5%, 1%, 2 and 5% and well dispersed in the molten CB.

Differential Scanning Calorimetry

DSC experiments were carried out at atmospheric pressure by using a Diamond apparatus (Perkin Elmer, Waltham, MA, USA). Samples (4.500-4.900 mg) were weighed into 50 µl aluminum pans and an empty pan was used as reference. The instrument was calibrated with reference to the melting temperatures and enthalpies of indium (Tm = 156.6 °C; ΔH = 28.45 J/g) and decane (Tm = -29.7 °C; ΔH = 202.1 J/g) standards. Dry nitrogen was used as purge gas in the DSC measurement chamber at a flow rate of 20 cm3/min. Thermograms were analyzed using Pyris software to obtain the enthalpy (J/g, integration of the DSC events) and transition temperatures T_{top} and T_{onset} (or T_{end}). T_{top} corresponded to the temperature at peak-top positions, whereas T_{onset} (or T_{end}) was defined as the temperature at intersections between baselines and tangents at inflection points of the initial (or final) peak slopes. A correction (described elsewhere[31]) was applied to the DSC thermograms based on cooling/heating rates different to 2°C/min, at which the instrument was calibrated.

During the measurements, samples were cooled from the melt of CB to -80 °C and subsequently heated both at constant rates selected from the combinations of 0.1, 0.5, 2, and 15 °C/min. The initial temperature was set to 55 °C for CB (without talc) to assure its complete melting or 80 °C for CB added with talc particles (referred to as CB + talc) to increase the fluidity of molten CB as a dispersion media for talc particles. For CB samples, three independent measurements were conducted for each experimental condition and the results were evaluated for random uncertainty with a 95% threshold of reliability using the Student's method.

For further interpretation of DSC thermograms, SR-XRD experiments were carried out under the same selected thermal treatments.

Synchrotron radiation X-ray diffraction

Structural change associated with polymorphic crystallization of CB was examined by SR-XRD experiments conducted on the beamline BL11-NCD-SWEET at the ALBA Synchrotron facility (Cerdanyola del Vallès, Barcelona, Spain). After sample-detector distance was fixed to 2.2 m, X-rays with an energy of 12.4 keV were applied to samples which were sealed in aluminum cells with Kapton polyimide film (DuPont, Wilmington, DE, USA) windows and then attached to a vertically placed thermal-control stage THMS600 (Linkam Scientific Instruments, Tadworth, UK). X-ray scattering data were collected on an ADSC detector with a pixel size of 103 μm x 103 μm for the small-angle X-ray diffraction (SAXD) data and on a LX255-HS Rayonix detector with a pixel size of 44 μm x 44 μm for the wide-angle X-ray diffraction (WAXD) data. The q-axis calibration was obtained by measuring silver behenate for SAXD and Cr2O3 for WAXD. The program pyFAI was used to integrate the 2D SAXD and 2D WAXD into the 1D data.[32]

Synchrotron radiation microbeam X-ray diffraction

Lamellar-plane directions of CB crystals occurring with talc addition were examined by SR-μ-XRD experiments conducted on the beamline BL46XU at the synchrotron radiation facility SPring-8 (Hyogo, Japan). After sample-detector distance was fixed to 0.483 m, a microbeam focusing X-rays with an energy of 12.4 keV to a size of 3 μm was applied to thin layered samples (CB + 0.1% talc and CB + 0.5% talc) which were sandwiched between two thin Mylar polyester films (DuPont Teijin Films U.S., Chester, VA, USA) and then attached to a vertically placed thermal-control stage LK-600PM (Linkam Scientific Instruments, Tadworth, UK). X-rays scattered from the samples were received as 2D area images by a PILATUS 2M detector (Dectris, Baden-Daettwil, Switzerland) both for SAXD and WAXD, with a camera distance of

483 mm. For larger scale area mapping, the 2D images to be merged were acquired while each sample was moved with a stepping motor in multiple steps at regular intervals of 3 μm under monitoring with an optical microscope. All the images were taken for the samples which were cooled at −50 °C after cooling from 80 °C at a rate of 15 °C/min.

RESULTS AND DISCUSSION

1. Polymorphism of bulk CB and containing talc at varying cooling/heating conditions

1.1. Rapid (15 °C/min) cooling and rapid (15 °C/min) and slow (0.5 °C/min) heating

CB samples in bulk and containing talc particles at concentrations from 0.1% to 5% were subjected to different dynamic thermal treatments by cooling from 80 °C (far above the melting temperature of CB) and reheating at different rates. Figure 1 shows the DSC thermograms obtained when CB and CB + 0.1%; 0.5%; 1%; 2% or 5% talc were cooled from the melt (Figure 1a, left) and subsequent heated (Figure 1a, right) at 15°C/min. Additionally, complementary SR-XRD data are detailed for CB in bulk (Figure 1b) and CB + 0.5% (Figure 1c) and 1% (Figure 1d) talc.

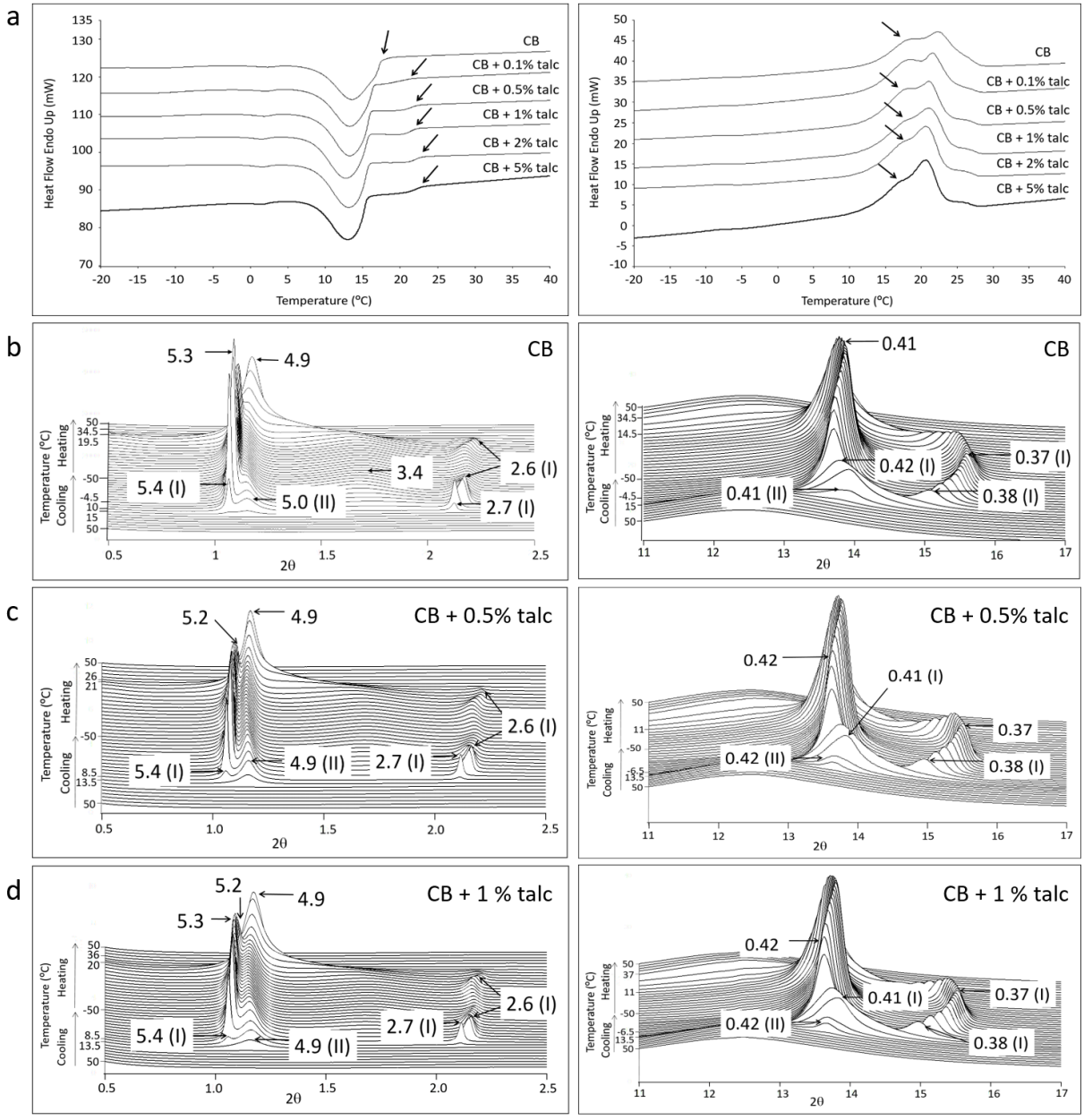

Figure 1. Effect of adding talc particles at different concentrations on DSC and SR-XRD results of bulk CB and CB + talc, taken under cooling and subsequently heating both at a rate of 15 °C/min. a) DSC cooling (left) and heating (right) thermograms and b-d) Time-course SAXD (left) and WAXD (right) profiles of SR-XRD data: b) bulk CB, c) CB + 0.5% talc, and d) CB + 1% talc. Unit: nm.

Forms II and I of CB crystallized from the melt in bulk state, and they were identified by typical SR-XRD peaks at 5.0 and 0.41nm; and 5.4, 2.7, 0.42 and 0.38nm, respectively. According to the corresponding DSC exothermic signal, this concurrent crystallization process initiated at 16.6 ± 0.5 °C (T_{onset}) and its peak top temperature was set at 13.5 ± 0.8 °C. The DSC cooling thermogram also exhibited a weak exothermic peak at 2.1 ± 0.6 °C, although no changes were detected in the SR-XRD patterns. During subsequent heating step at 15 °C/min, Forms II and I crystals simply melted, so that corresponding SR-XRD peaks vanished. Endothermic DSC phenomena with peak top temperatures of 18.0 ± 1.5 °C and 22.3 ± 1.4 °C were assigned to Forms I and II melting, respectively. A shoulder was located at 27.2 ± 1.1 °C and end melting temperature was set at 27.7 ± 1.1 °C. These experimental conditions for bulk CB were already reported by our group in previous work.[6]

Selected crystallization and melting temperatures for CB in bulk and CB + talc at different concentrations are gathered in Table 1.

Table 1. Crystallization and melting temperatures (°C) of bulk CB and CB + talc (T) at different concentrations when cooled at 15 °C/min and heated at 15 and 0.5 °C/min. The letters *c* and *m* represent crystallization and melting, respectively.

	Cooling at 15 °C/min			Heating at 15 °C/min			
	II + I (*c*)			I (*m*)	II (*m*)		
	T_{onset}	T_{top} 1	T_{top} 2	T_{top}	T_{top}		
CB	16.6 ± 0.5		13.5 ± 0.8	18.0 ± 1.5	22.3 ± 1.4		
CB + 0.1% T	20.9	18.7	13.3	18.5	21.6		
CB + 0.5% T	22.6	20.2	13.3	18.4	21.2		
CB + 1% T	22.1	20.2	12.8	17.9	21.1		
CB + 2% T	22.9	21.1	13.2	17.6	20.7		
CB + 5% T	23.2	21.3	13.0	17.4	20.6		
				Heating at 0.5 °C/min			
				I → III + IV	II (*m*)	III (*m*)	IV (*m*)
				T_{top}	T_{top}	T_{top}	T_{top}
CB				19.3 ± 0.5	22.3 ± 0.6	27.2 ± 0.3	32.0 ± 0.5
CB + 0.1% T				18.2	22.2	26.6	31.7
CB + 0.5% T				18.3	22.7	26.8	31.6
CB + 1% T				18.2	22.5	27.0	31.5
CB + 2% T				18.4	23.5	27.6	32.4
CB + 5% T				18.1	22.6	26.9	31.5

As talc was added, onset crystallization temperature significantly increased (from about 16.6 °C for CB to 23.2 °C for CB with 5% talc), due to the occurrence of an additional peak (see arrows in Figure 1a left). Regarding SR-XRD data, the sequence of polymorphic crystallization and melting was not altered with the inclusion of talc particles in CB. However, one may note an increase of Form II peaks intensity (specially that at 4.9 nm) at the expense of Form I (5.4 nm) for talc concentrations of 0.5% and 1% in CB (see Figures 1c and 1d). This stabilization of more stable Form II with the addition of talc was also evidenced by the intensity decrease of the DSC

endothermic event corresponding to the melting of less stable Form I, pointed by arrows in Figure 1a (right).

Samples were also subjected to slow heating process (0.5 °C/min) after rapid cooling at a rate of 15 °C/min, as depicted in Figure 2.

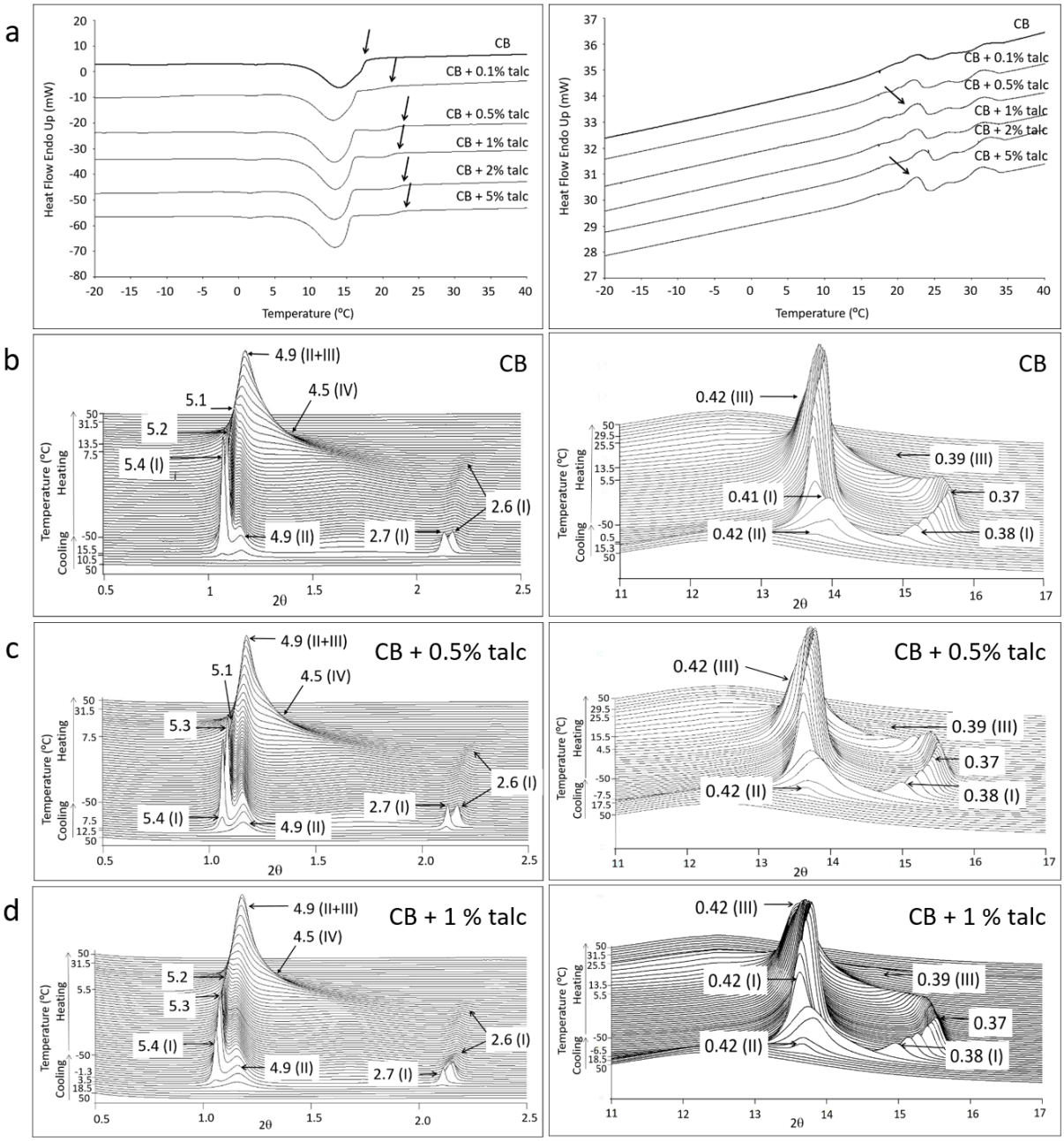

Figure 2. Effect of adding talc particles at different concentrations on DSC and SR-XRD results of bulk CB and CB + talc, taken under cooling at a rate of 15 °C/min and subsequently heating at 0.5 °C/min. a) DSC cooling (left) and heating (right) thermograms and b-d) Time-course SAXD (left) and WAXD (right) profiles of SR-XRD data: b) bulk CB, c) CB + 0.5% talc, and d) CB + 1% talc. Unit: nm.

By slowly heating Forms II and I crystals formed by cooling at 15 °C/min, SR-XRD data revealed the extinction of Form I peaks at 5.1 and 2.6 nm (shifted from those at 5.4 and 2.7 nm) and a simultaneous intensity decrease of the SR-WAXD peak at 0.42 nm at a temperature range between 7.5 and 13.5 °C (see Figure 2b and enlarged SR-XRD patterns in Supporting Information Figure S1). Then, peaks at 4.9 nm (having a shoulder at 4.5 nm) and 0.42 nm straightaway became more intense and additional peak at 0.39 nm occurred. These changes may be due to a complex polymorphic transformation from Form I to Forms III and IV. This polymorphic transition may be related to the first endothermic DSC event with top temperature of 19.3± 0.5 °C (Figure 2a right and Table 1). As bulk CB was further heated, melting of Forms II, III and IV occurred, processes which were associated to endothermic DSC signals at 22.3 ± 0.6 °C, 27.2 ± 0.3 °C, and 32.0 ± 0.5 °C, respectively. According to SR-XRD patterns, no peaks were present at 31.5 °C.

The addition of talc caused a shifting of the onset crystallization temperature to higher temperatures, as detailed above for cooling and heating conditions at 15 °C/min. Furthermore, corresponding DSC heating curves exhibited a higher definition of endothermic peak at around 22 °C due to the intensity decrease of previous signal at 18 °C as talc concentration increased from 0.1% to 5% (see arrows in Figure 2a, right). Regarding SR-XRD data, Figures 2c and 2d show patterns obtained for added talc concentrations of 0.5% and 1%. One may note the change in the SR-SAXD profiles that the peak for Form II (d = 4.9 nm) developed at the expense of that for

Form I (d = 5.4 nm) as talc concentration increased. Moreover, higher amount of Form III (note peak at 0.42) also occurred during heating when increasing talc concentration (see lateral views of corresponding SR-XRD in Supporting Information Figure S2). All these effects became more significant for CB + 1% talc. Regarding DSC heating curves, the last endothermic signal corresponding to the melting of Form IV crystals became more intense at higher talc concentrations.

1.2. Intermediate (2 °C/min) cooling and heating

CB in bulk and CB + talc samples were also exposed to cooling and heating procedures at 2 °C/min. Figure 3 shows DSC cooling and heating curves, and SR-XRD patterns for bulk CB and CB containing 0.5 and 1% talc. Typical phase transition temperatures of CB in these samples determined for the DSC exothermic and endothermic peaks are summarized in Table 2.

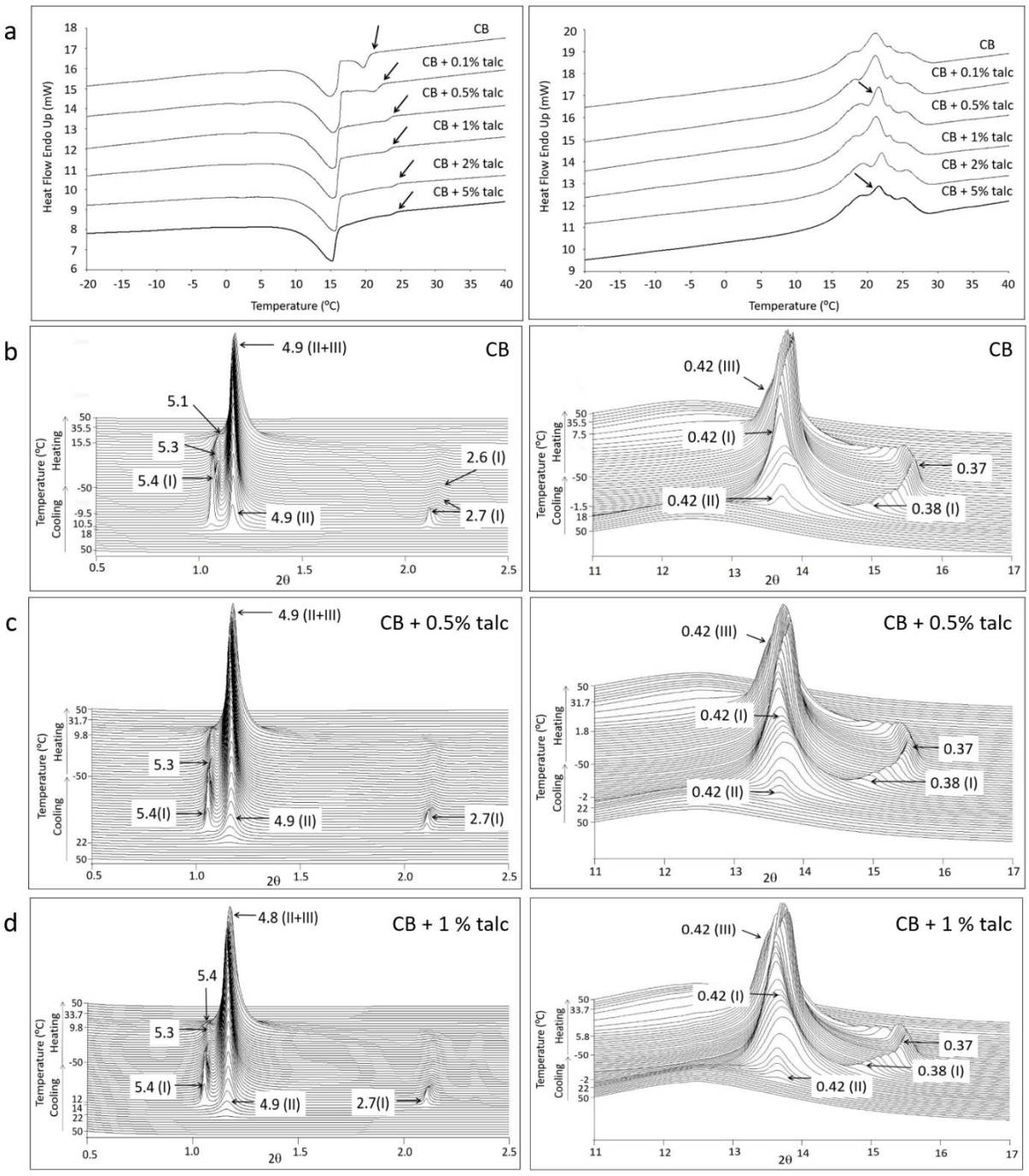

Figure 3. Effect of adding talc particles at different concentrations on DSC and SR-XRD results of bulk CB and CB + talc, taken under cooling and subsequently heating both at a rate of 2 °C/min. a) DSC cooling (left) and heating (right) thermograms and b-d) Time-course SAXD (left) and

WAXD (right) profiles of SR-XRD data: b) bulk CB, c) CB + 0.5% talc, and d) CB + 1% talc. Unit: nm.

Table 2. Crystallization, polymorphic transformation and melting temperatures (°C) of bulk CB and CB + talc (T) at different concentrations when cooled and heated at 2 °C/min. The letters *c* and *m* represent crystallization and melting, respectively.

	Cooling at 2 °C/min			Heating at 2 °C/min		
	II (*c*)		I (*c*)	I → III	II (*m*)	III (*m*)
	T_{onset}	T_{top}	T_{top}	T_{top}	T_{top}	T_{top}
CB	21.1 ± 1.8	19.7 ± 0.5	15.2 ± 0.9	18.1 ± 1.5	21.3 ± 0.6	26.0 ± 0.9
CB + 0.1% T	22.3	21.1	15.4	18.3	21.1	25.7
CB + 0.5% T	23.8	22.7	15.3	19.1	21.6	25.5
CB + 1% T	23.7	22.7	15.4	19.3	21.7	25.6
CB + 2% T	25.0	23.6	15.6	19.5	22.0	25.8
CB + 5% T	25.0	23.6	15.2	19.2	21.6	25.3

When CB was cooled, initial crystallization temperature (T_{onset}) was set at 21.1 ± 1.8 °C and two main independent exothermic DSC events with peak top temperatures at 19.7 ± 0.5 °C and 15.2 ± 0.9 °C were observed. These signals were again attributed to the crystallization of CB in Forms II and I, respectively. Form II was identified by small- and wide-angle peaks at 4.9 and 0.42 nm, whereas SR-XRD characteristic peaks of Form I occurred at 5.4, 2.7, 0.42 and 0.38 nm.

By reheating the sample from -80 °C to 55 °C, synchrotron data revealed the extinction of Form I-specific SR-SAXD peaks for d = 5.4 and 2.7 nm at around 15 °C, and an intensity decrease of SR-WAXD peak at 0.42 nm. This was followed by an intensity increase of peaks at 4.9 and 0.42

nm, which corresponded to the first DSC endothermic signal with top temperature of 18.1 ± 1.5 °C probably due to the Form I → Form III polymorphic transformation. Soon after, Forms II and III melted (endothermic DSC events at 21.3 ± 0.6 °C and 26.0 ± 0.9 °C, respectively), and no SR-XRD peaks were present at 35.5 °C.

Once again, the addition of talc caused a meaningful increase of the onset crystallization temperature, changing T_{onset} from 21.1 °C for bulk CB to 25.0 °C for CB + 2% or 5% talc (see Figure 3a and Table 2). Regarding the DSC heating curves, the melting peak of Form II (T_{top} = 21.3 ± 0.6 °C) slightly decreased in intensity with increasing talc concentration, as indicated by arrows in Figure 3a right. This stabilization of more stable forms caused by the inclusion of talc was again evident in SR-XRD patterns. During cooling, the SR-SAXD peak intensity of Form II (4.9 nm) increased at the expense of Form I peak (5.4 nm) as talc was added and, when samples were subsequently heated, characteristic Form III SR-WAXD peak at 0.42 nm became more intense for talc concentrations of 0.5% and 1% (see Figures 3c right, and 3d right).

1.3. Slow (0.5 °C/min) cooling and intermediate (2 °C/min) heating

Resemblant polymorphism was monitored when samples were cooled from the melt at a lower rate of 0.5 °C/min and reheated at 2 °C/min (Figure 4 and Table 3).

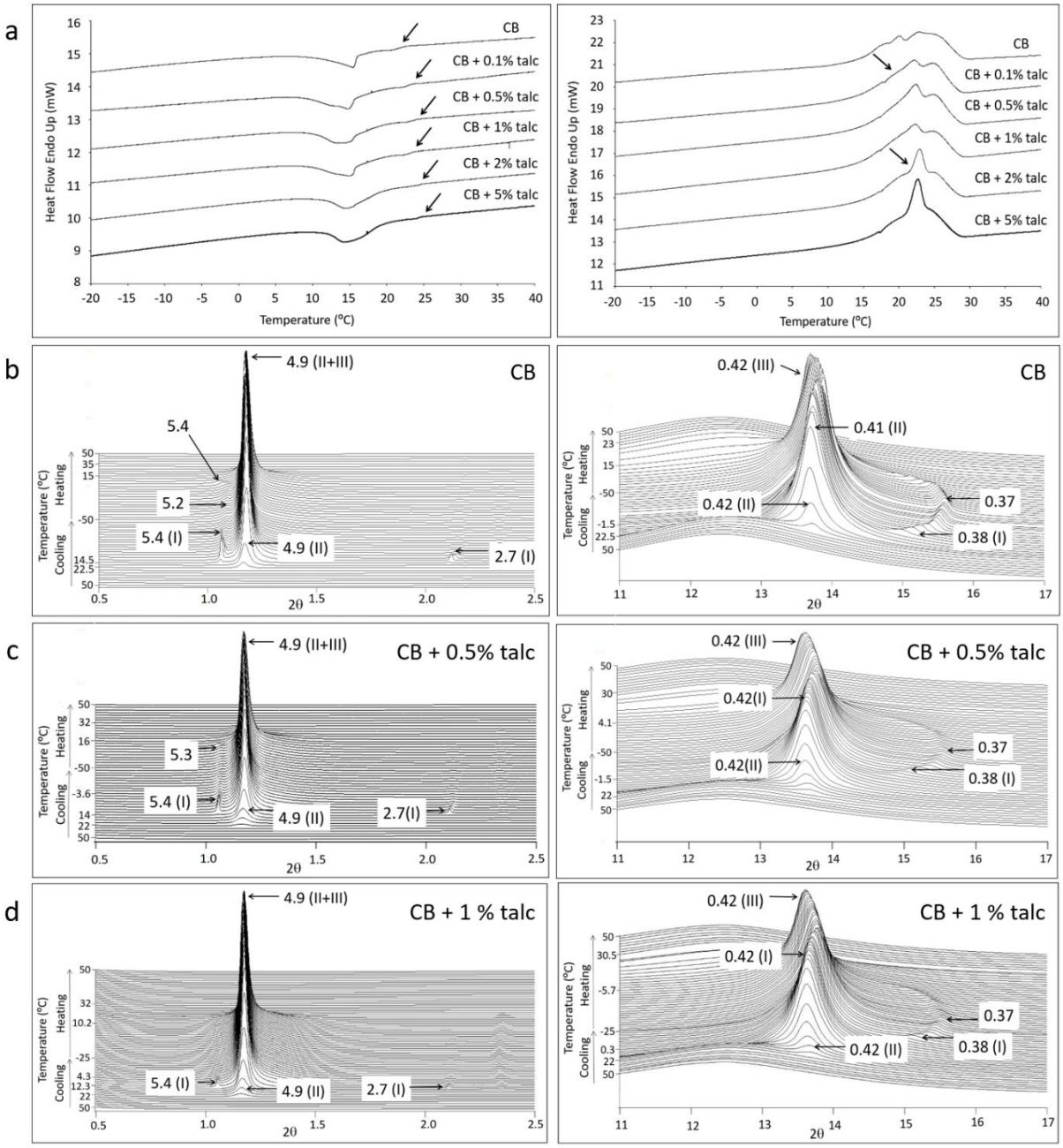

Figure 4. Effect of adding talc particles at different concentrations on DSC and SR-XRD results of bulk CB and CB + talc, taken under cooling at a rate of 0.5 °C/min and subsequently heating at a rate of 2 °C/min. a) DSC cooling (left) and heating (right) thermograms and b-d) Time-course SAXD (left) and WAXD (right) profiles of SR-XRD data: b) bulk CB, c) CB + 0.5% talc, and d) CB + 1% talc. Unit: nm.

Table 3. Crystallization, polymorphic transformation and melting temperatures (°C) of bulk CB and CB + talc (T) at different concentrations when cooled at 0.5 °C/min and heated at 2 °C/min. The letters *c* and *m* represent crystallization and melting, respectively.

	Cooling at 0.5 °C/min			Heating at 2 °C/min		
	II (*c*)		I (*c*)	I → III	II (*m*)	III (*m*)
	T_{onset}	T_{top}	T_{top}	T_{top}	T_{top}	T_{top}
CB	22.8 ± 1.1	21.0 ± 0.6	15.7 ± 0.7	20.4 ± 0.9	23.0 ± 0.6	25.3 ± 0.7
CB + 0.1% T	23.4	22.3	14.8	19.4	22.2	24.9
CB + 0.5% T	24.2	22.5	14.2	19.7	22.4	24.9
CB + 1% T	24.5	22.6	15.0	19.9	22.3	24.8
CB + 2% T	24.6	23.3	14.7	20.3	22.9	25.0
CB + 5% T	24.7	24.0	14.6	20.0	22.6	25.0

Onset crystallization temperature was set at 22.8 ± 1.1 °C and, once more, Form II crystallized at first (peak top T of 21.0 ± 0.6 °C), which was identified by SR-SAXD and -WAXD peaks at 4.9 and 0.42 nm, respectively, and, straightaway, less stable Form I (SR-XRD peaks at 5.4, 2.7, 0.42 and 0.38 nm) occurred (15.7 ± 0.7 °C). By comparing SR-XRD peaks of Form I in previous experimental conditions, one may note that fewer amount of Form I was crystallized as the cooling rate decreased from 15 °C/min to 2 °C/min and 0.5 °C/min. When crystallized CB was thereafter heated at 2 °C/min, diffraction peaks at 5.4 and 2.7 nm vanished at approximately 15 °C and peaks with d-spacing values of 4.9 and 0.42 nm very slightly increased in intensity, due to a polymorphic transformation from Form I to Form III. However, this increase was not as significant as for previous experiments of cooling-heating at 15 °C/min-0.5 °C/min and 2 °C/min-2 °C/min, as the amount of metastable Form I obtained was higher at these conditions. Conversely, when bulk CB

was cooled at 0.5 °C/min and heated at 2°C/min, a continuous intensification of the SR-WAXD peak at 0.42 was observed, probably due to an ongoing formation of Form III during heating. The Form I → Form III polymorphic transformation was assigned to the first main endothermic DSC event with top temperature of 20.4 ± 0.9 °C. On further heating, Forms II and III melted at 23.0 ± 0.6 °C and 25.3 ± 0.7 °C, respectively, according to the DSC data. At 35 °C, neither the SR-SAXD nor the SR-WAXD pattern presented diffraction peaks.

With the addition of talc, and similarly to previous experimental conditions, onset crystallization temperature increased (from 22.8 °C for CB bulk to 24.7 °C in CB + 5% talc), as shown in Figure 4a (left) and Table 3. As to DSC heating curves (Figure 4a, right), the endothermic signal at 20.4 ± 0.9 °C, assigned to the Form I → Form III polymorphic transformation, became less important as talc was added, which might be due to a decrease in the amount of Form I obtained. Then, DSC heating curves evolved into simpler thermograms with sharper endothermic event at around 23 °C (Form II melting) at increasing talc concentrations. SR-XRD likewise revealed a decrease of the intensity of SR-SAXD peak at 5.4 nm (Form I) while that at 4.9 nm (Forms II and III) increased with talc addition. However, the effects caused by talc at these experimental circumstances were not as meaningful as for previously detailed cooling-heating conditions of 15 °C/min-15 °C/min, 15 °C/min – 0.5 °C/min, and 2 °C/min – 2 °C/min, at which higher amounts of metastable form I were initially crystallized, as will be discussed further on.

1.4. Slow (0.1 °C/min) cooling and rapid (15 °C/min) heating

Finally, the lowest cooling rate of 0.1 °C/min followed by a rapid heating procedure at 15 °C/min was applied to CB in bulk state and CB samples containing talc particles (see Figure 5 and Table 4).

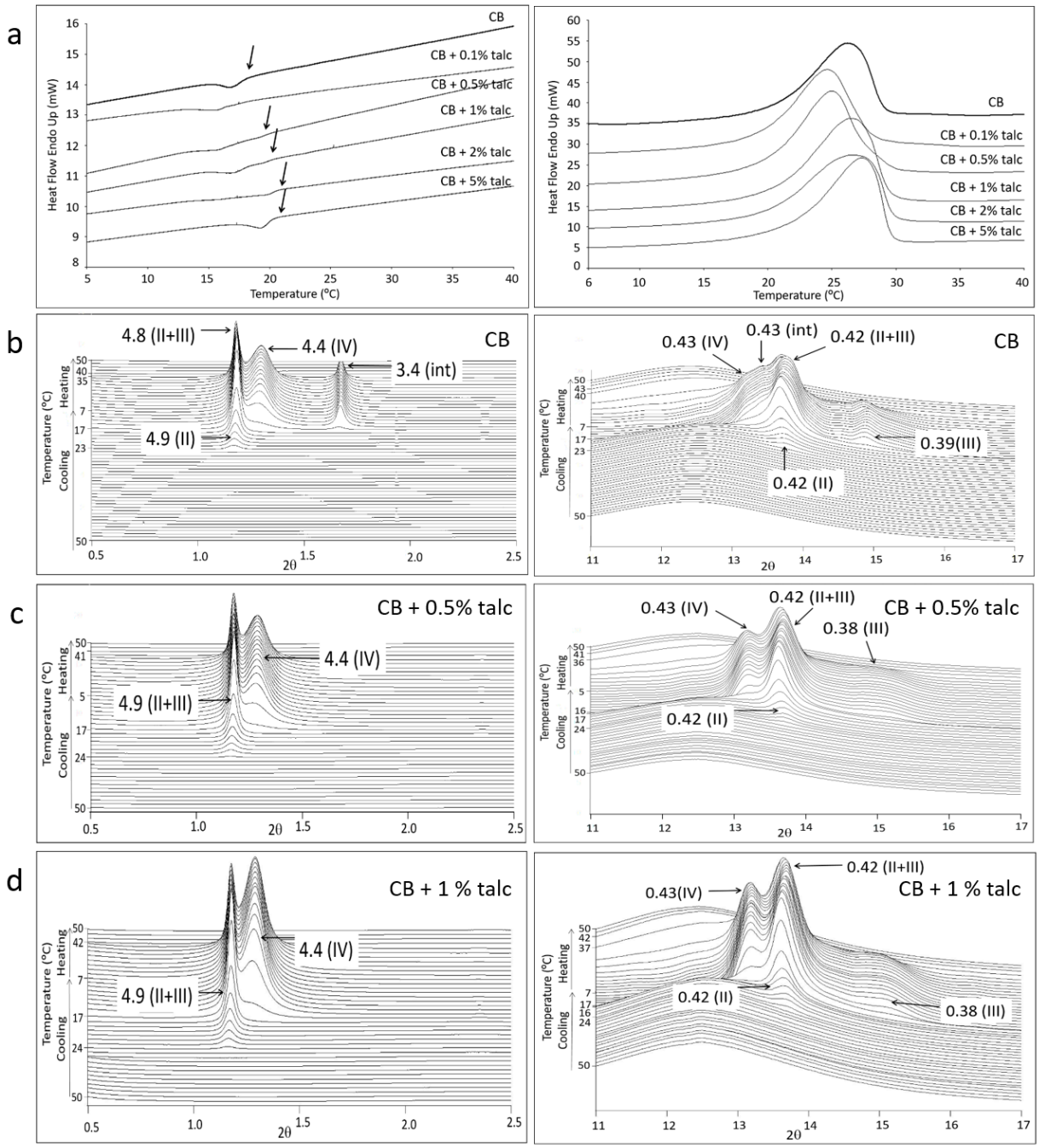

Figure 5. Effect of adding talc particles at different concentrations on DSC and SR-XRD results of bulk CB and CB + talc, taken under cooling at a rate of 0.1 °C/min and subsequently heating at a rate of 15 °C/min. a) DSC cooling (left) and heating (right) thermograms and b-d) Time-course

SAXD (left) and WAXD (right) profiles of SR-XRD data: b) bulk CB, c) CB + 0.5% talc, and d) CB + 1% talc. Unit: nm.

Table 4. Crystallization, polymorphic transformation and melting temperatures (°C) of bulk CB and CB + talc (T) at different concentrations when cooled at 0.1 °C/min and heated at 15 °C/min. The letters *c* and *m* represent crystallization and melting, respectively.

	Cooling at 0.1 °C/min		Heating at 15 °C/min	
	II + III + IV (*c*)		II + III + IV (*m*)	
	T_{onset}	T_{top}	T_{onset}	T_{top}
CB	18.6 ± 0.7	17.0 ± 0.7	19.7 ± 1.0	26.5 ± 0.8
CB + 0.1% T	18.9	15.7	18.7	24.7
CB + 0.5% T	20.1	15.9	18.2	25.1
CB + 1% T	20.4	17.0	19.1	26.6
CB + 2% T	20.8	19.6	18.4	26.6
CB + 5% T	20.5	19.3	19.6	27.3

By cooling bulk CB at such a low rate, CB did not crystallize in the least stable Form I, and the SR-XRD data revealed, at around 23 °C, the occurrence of Form II diffraction peaks at 4.9 and 0.42 nm. Next, a SR-SAXD peak for d = 4.4 nm and SR-WAXD peaks for d = 0.43 and 0.39 nm occurred at 17 °C, indicating concurrent crystallization in Forms III and IV. Just at the same time, the other SR-XRD peaks for d = 3.4 and 0.43 nm occurred alone, which were attributed to a feasible intermediate (int) phase evolved from Form II of CB crystals[3] and similar to the peaks for the metastable structure of SOS crystals with mixed double-chain and triple-chain (2L + 3L) packing.[33] The related DSC cooling curve displayed a single broad exothermic event with T_{onset} = 18.6 ± 0.7 °C and T_{top} = 17.0 ± 0.7 °C. When crystallized CB was heated to 55 °C at 15 °C/min,

the resulting CB crystals in Forms II, III and IV, as well as in the intermediate phase simply melted, due to the high rate used. Then, all SR-XRD peaks vanished practically simultaneously, and at 40 °C no signals were present. This melting process was evidenced by a single broad endothermic DSC phenomenon, with T_{onset} = 19.7 ± 1.0 °C and T_{top} = 26.5 ± 0.8 °C (Table 4).

As shown in Figures 5c and 5d, the polymorphic behavior of samples containing talc particles at different concentrations were essentially the same under the slowest cooling at a rate of 0.1 °C/min. However, significant variations in the relative amount of the occurring phases were reflected particularly on the change in the DSC heating thermogram and that in the SR-XRD peak patterns as follows. In the DSC heating thermograms (Figure 5a right), the T_{top} once dropped with 0.1% talc addition rose with increasing concentration of talc particles: specifically, T_{top} = 26.5 ± 0.8 °C (CB in bulk), 24.7 °C (CB + 0.1% talc), 25.1 °C (CB + 0.5% talc), 26.6 °C (CB + 1% talc and CB + 2% talc), and 27.3 °C (CB + 5% talc). For the SR-XRD peak patterns (Figures 5c and 5d), the Form IV specific peaks for d = 4.4 and 0.43 nm increased with respect to the Forms II + III specific peaks for d = 4.9 and 0.42 nm, indicating that crystallization in Form IV was enhanced with increasing concentration of talc particles. In addition, T_{onset} of the exothermic peak in the DSC cooling thermogram (Figure 5a left) appeared to increase from 18.6 ± 0.7 °C (CB in bulk) to 18.9 °C (CB + 0.1% talc), 20.1 °C (CB + 0.5% talc), 20.4 °C (CB + 1% talc), 20.8 °C (CB + 2% talc), and 20.5 °C (CB + 5% talc); this indicates that crystallization in Form II was also promoted by adding talc particles. Furthermore, it should be payed particular attention that crystallization in the intermediate phase did not occur with 0.1% and 0.5% talc addition.

1.5. Summary and discussion of the polymorphic behavior

As a summary, Figure 6 shows polymorphic crystallization and transformation processes determined for CB in bulk and containing talc particles when subjected to different cooling/heating conditions.

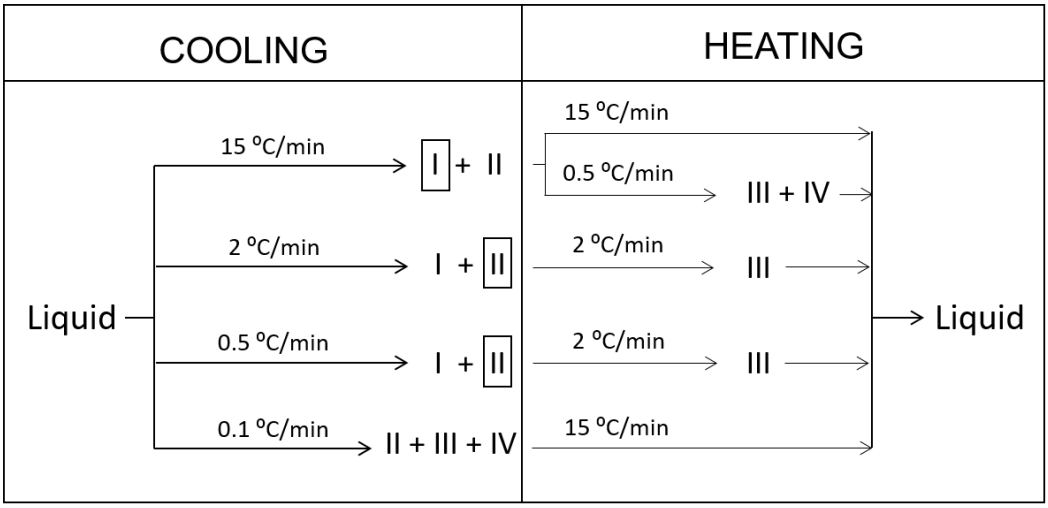

Figure 6. Polymorphic crystallization and transformation of bulk CB, and CB + 0.5% or 1% talc when subjected to different cooling and heating conditions.

As demonstrated in previous work with single TAG components, higher cooling/heating rates leaded polymorphic processes to attain less stable forms, while gentler conditions permitted the predominance of more stable phases.[34-37] However, it should be noted that, in general, by tailoring specific dynamic thermal treatments, pure triacylglycerols exhibited a high ability to achieve most stable polymorphs by decreasing the rates of cooling/heating, whereas CB became more reticent to evolve,[6] similarly to 1,3-dipalmitoyl-2-oleoyl glycerol,[35] which is one of the main TAGs of CB.

When molten CB was cooled at different rates of 15, 2 and 0.5 °C/min, concurrent crystallization of Forms I and II was determined. The relative intensity of SR-SAXD peaks in Figures 1, 3 and 4

evidenced that Form I predominated in front of Form II when the highest cooling rate of 15 °C/min was applied. However, Form II became more dominant at lower speeds of 2 and 0.5 °C/min. By contrast, complex concurrent crystallization of Forms II, III and IV took place at the lowest rate applied (0.1 °C/min).

Regarding the heating rates variation, highest speed of 15 °C/min caused the straightforward melting of the previously crystallized polymorphs. Then, Forms I and II obtained by cooling at 15 °C/min, but also Forms II, III and IV crystallized at 0.1 °C/min, simply melted when they were heated at 15 °C/min. Contrarily, the use of lower heating rates of 2 and 0.5 °C/min resulted in the polymorphic transformation to more stable forms before the melting. Then, Form III occurred when Form I and II crystals were heated at 2 °C/min, whereas Form IV was also reached at 0.5 °C/min.

Within this scenario, the addition of talc played a significant role as polymorphic stabilizer, since it increased the amount of more stable polymorphs attained at the expense of less stable forms, and these effects became more important for talc concentrations of 1%. In more detail, for concurrent crystallization processes of Forms I and II, the addition of talc provoked an increase of the amount of Form II obtained, at the expense of least stable Form I. As to polymorphic transformation during heating, higher amounts of Form III occurred when talc concentration was increased, as corresponding SR-XRD intensity peaks disclosed. Finally, at gentler conditions of very slow cooling (0.1 °C/min), at which concurrent crystallization of Forms II, III and IV happened, talc promoted the occurrence of more stable Form IV, and it also avoided the development of the intermediate form detected in CB bulk.

These promoting and stabilizing influences of talc became more meaningful when high cooling rates were used, as depicted in Figure 7. Here, the variation of the amount of crystallizing Forms

I and II at the different talc concentrations is represented through the ratio of Form I and Form II SR-SAXD peaks at 5.4 and 4.9 nm, respectively.

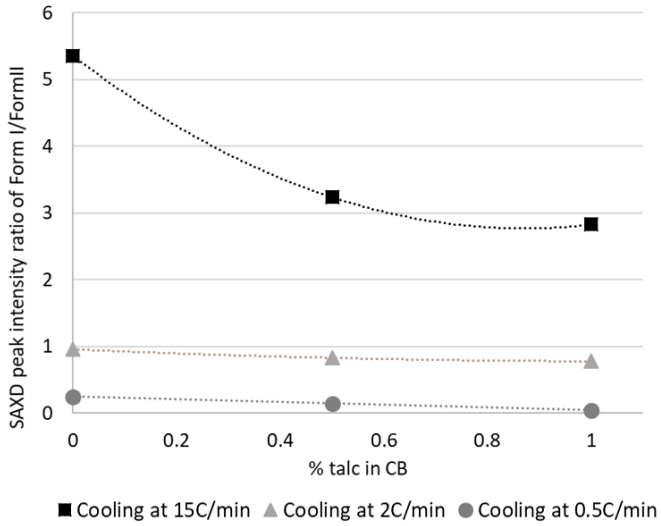

Figure 7. Variation in the amount of crystallizing Forms I and II of CB when increasing talc concentration through the ratio of peaks intensity.

At conditions of 0% talc, proportions of intensities of peaks of Forms I and II were higher for cooling rates of 15 °C/min and lower for 2 and 0.5 °C/min, due to higher amounts of Form I obtained at the highest speed used. Then, proportions decreased with talc concentrations of 0.5% and 1% and drops became more intense for experimental conditions at which a cooling rate of 15 °C/min was employed. The effects were clearly noticeable for talc concentrations of 0.5%. Talc particles acted as heterogeneous nucleation sites, and it seems that promoting influences were more effective at high cooling rates conditions, when higher amounts of least stable Form I were

crystallized which, due to its high metastability, may be more easily stabilized by talc. As more stable polymorphs were reached, stabilizing influences of talc were not as fruitful.

These effects were also confirmed regarding the Form I → Form III polymorphic transformation. As previously stated, talc exerted more important stabilizing effects of Form III for experimental conditions of 15 °C/min-15 °C/min, 15 °C/min – 0.5 °C/min, and 2 °C/min – 2 °C/min, than for 0.5 °C/min-2 °C/min, at which fewer amounts of Form I initially crystallized due to the low cooling rate applied.

Talc also caused a relevant increase of the onset crystallization temperature at all experimental conditions. The differences between CB in bulk and containing 5% talc for cooling rates of 15, 2, 0.5 and 0.1 °C/min were of about 7, 4, 2 and 2 °C, respectively. The variation of onset crystallization temperature of CB samples in bulk state and containing talc particles at the different concentrations are represented in Figure 8 for cooling rates of 15, 2 and 0.5 °C/min.

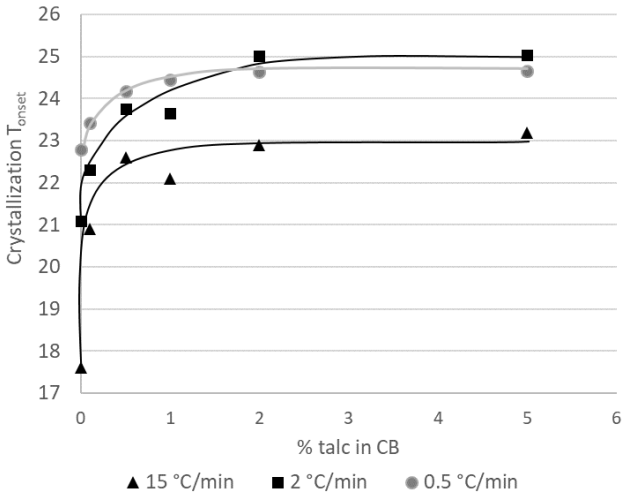

Figure 8. Variation of onset crystallization temperature of CB and CB + talc at different concentrations (0.1%, 0.5%, 1%, 2% and 5%) when crystallized at different rates of cooling (15, 2, and 0.5 °C/min)

Onset temperatures exhibited logarithmic growth type in all cases, so that most important variations were detected at talc concentrations lower than 1%. From 1 to 5% talc, onset crystallization temperatures were not as meaningful. Additionally, one may note that, once more, talc effects became more significant for highest cooling rate conditions of 15 °C/min, as the addition of just 0.1% talc already caused an increase of about 4 °C (see also Table 1). By contrast, at a lower cooling rate of 0.5 °C/min, no significant differences were observed when 0.1% talc was added to CB (solely 0.6 °C, which may be within experimental error). However, more important increase (of about 1.4 °C) occurred at 0.5% talc (Table 3).

2. Lamellar plane arrangements of TAG molecules on talc particles surface

2.1. SR-μ-XRD patterns of CB containing 0.5 and 0.1% talc

Based on the DSC and SR-XRD results that CB crystallization in more stable forms was promoted even when 0.1% talc particles were added to CB and cooled at the highest rate of 15 °C/min, SR-μ-XRD experiments were performed to determine how TAG molecules interact with talc, that is to elucidate the adsorption mode for heterogeneous nucleation of TAG molecules on talc particles surface. We determined that a 0.5%, and even a 0.1% talc was sufficient to significantly increase onset crystallization temperatures or to observe some stabilization of polymorphic forms. By taking this into account, SR-μ-XRD experiments were carried out on CB samples including 0.5 and 0.1% talc, after cooling at 15 °C/min. Figure 9 shows SR-μ-XRD patterns (SAXD data) taken at 256 individual positions of crystallized CB containing 0.5% talc after cooled at 15 °C/min. Mapping of analyzed samples were carried out with steps of 3 μm, which is the distance between patterns.

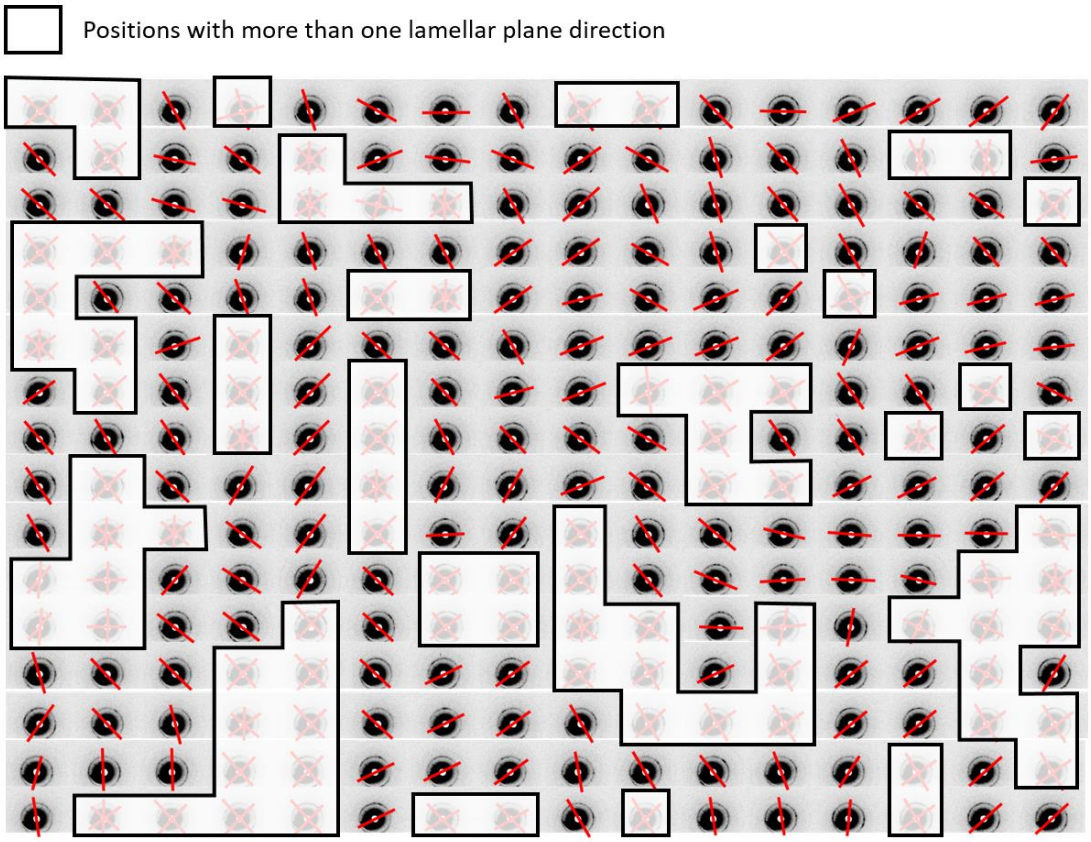

Figure 9. Area mapping of SR-μ-XRD 2D patterns (SAXD data) with lamellar plane directions (red lines) of CB crystals occurring in CB + 0.5% talc, taken at -50 °C after cooling at a rate of 15 °C/min.

One may observe that all the analyzed positions exhibited clear diffraction arc peaks in all the areas in which microbeam was irradiated. Within each pattern, the orientation of diffraction peaks permits to determine the lamellar direction of TAG crystals through the azimuthal angle (χ) extension, as explained in previous work.[25] Then, we concluded that lamellar planes of TAG crystals at each position were aligned along the direction denoted by red lines in Figure 9.

However, not all the analyzed positions were based on one markedly lamellar plane direction, but the co-existence of two or more. In this case, one may consider that crystals had a randomly oriented lamellar arrangement. These positions with random alignment are those located in whitish areas in the figure. As shown, in 88 spots over the 256 analyzed, TAG crystals were randomly oriented. Among the positions with one lamellar plane orientation, this alignment was changing in the different patterns taken in the two dimensions of the scanned sample. Then, a possible explanation of the oscillation of the lamellar plane direction and the existence of certain areas with random orientation is that arbitrarily dispersed talc particles may be located close to the positions with random orientation.

SR-μ-XRD was also applied to CB containing 0.1% talc, under the same experimental conditions (Figure 10).

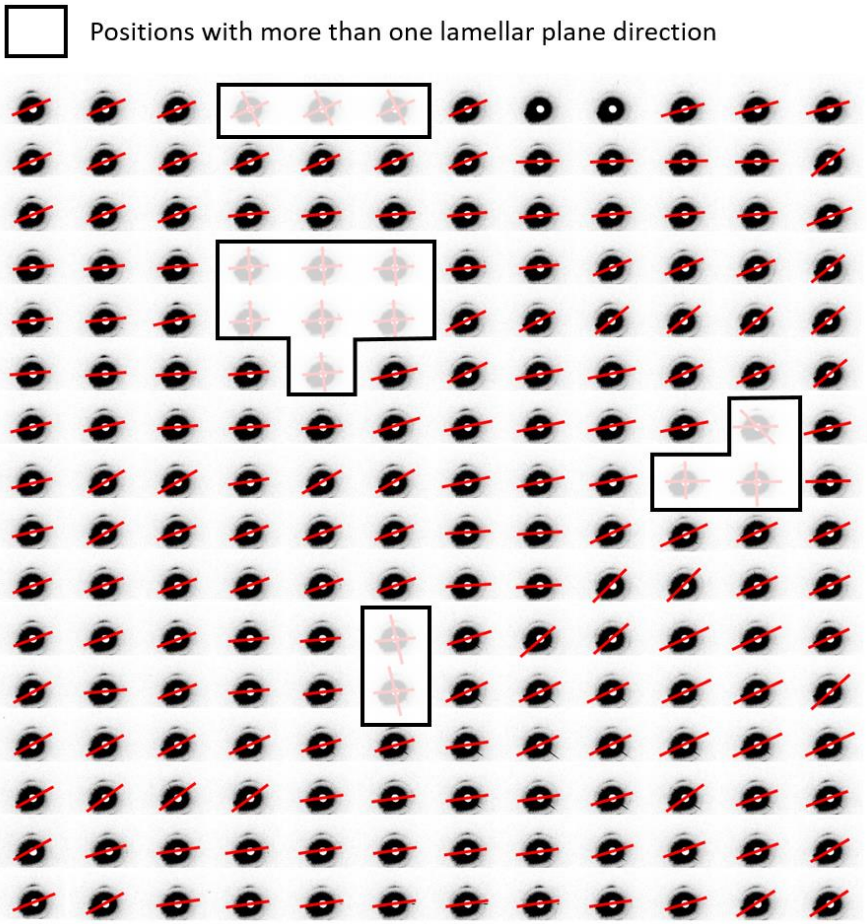

Figure 10. Area mapping of SR-μ-XRD 2D patterns (SAXD data) with lamellar plane directions (red lines) of CB crystals occurring in CB + 0.1% talc, taken at -50 °C after cooling at a rate of 15 °C/min.

In this case, SR-μ-XRD spots were more defined, that is to say, arc peaks became narrower than those observed at 0.5% talc. Among the 192 individual patterns obtained, lamellar planes were clearly aligned in 177, and random orientation was found in just 15 positions. Another relevant characteristic is that lamellar orientation was equivalent at the all positions analyzed, so that it was not specially oscillating through the two-dimensions of the sample. Then, one may conclude that the presence of only 0.1% talc particles in cocoa butter clearly showed the alignment of TAG

molecules through the lamellar plane direction, and this effect was much pronounced than at a higher concentration of 0.5% talc. As shown in Figure 9, a talc concentration of 0.5% caused too many interactions with TAG molecules, as confirmed by the high number of analyzed positions which exhibited more than one lamellar plane direction. Then, SR-µ-XRD may be too sensible technique for such high concentrations of talc.

2.2. Elucidation of a model

According to the SR-µ-XRD results, we defined a tentative model of TAGs molecules arrangement on talc particles surface, which may be described as follows.

In order to explain why TAGs lamellar orientation was equivalent at all individual positions at 0.1% talc concentration, one may also consider the disposition of the sample holder. As stated, each sample was set in a thin layer, between two Mylar films, and it was vertically oriented to perform SR-µ-XRD experiments while controlling temperature. Then, molten CB with dispersed talc particles crystallized after rapid cooling (15 °C/min). The vertical orientation of the sample may probably have forced talc particles to precipitate to the bottom before complete CB crystallization. Figure 11a illustrates the precipitation and/or dispersion of talc particles in the sample holder for low (0.1%, left) and higher (0.5%, right) talc concentrations.

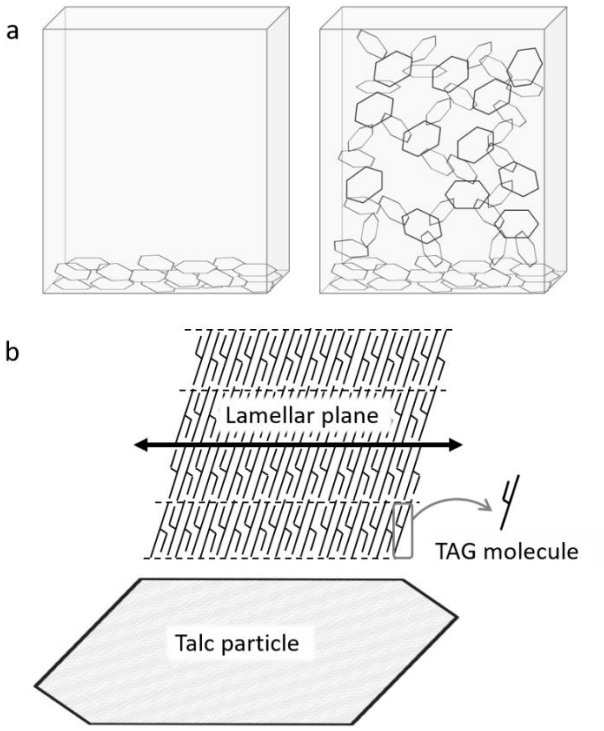

Figure 11. Postulated illustration of a) 0.1% (left) and 0.5% (right) talc particles dispersing in CB within SR-μ-XRD sample holders and b) arrangement of TAG molecules in CB crystals growing at talc particle surfaces.

For low talc concentrations, most of the flake-shaped talc particles may have precipitated and landed with their wide surface (that is the cleavage surface of talc) parallel to the horizontal direction. In this case, the direction of talc surface may coincide with the lamellar plane direction of TAG molecules. This was observed at all SR-μ-XRD patterns of CB containing 0.1% talc, where the parallel arrangement of lamellar planes in layers confirmed that TAG molecules may be adsorbed on cleavage surfaces of talc. By contrast, higher concentrations of talc particles may have partly formed random networks in bulk CB due to the increased contact frequency, resulting in the randomized lamellar plane direction of TAG molecules, as observed in the SR-μ-XRD patterns of CB containing 0.5% talc. Following our hypothesis, Figure 11b shows an illustration of molecular arrangements of TAGs on talc particles surface. As explained above, according to it, TAG

molecules may be aligned with their long axis normal to the cleavage surface of talc. Partial cleavage may bring talc particles step and kink sites onto which TAG molecules can be adsorbed. This interpretation was firstly proposed by Yoshikawa et al.[20] and this work confirmed it by using SR-μ-XRD techniques. However, we should stress again that this becomes a very tentative model and further research may be required to confirm its validity.

CONCLUSIONS

CB polymorphism was studied under dynamic conditions of varying cooling and heating rates in bulk state and including talc nanoparticles as minor component at concentrations of 0.1%; 0.5%; 1%; 2% and 5%. More stable polymorphic forms predominated at low cooling and heating rates and, additionally, the inclusion of talc also played a significant role as polymorphic stabilizer, as the amount of more stable forms were intensified at the expense of less stable forms for increasing talc concentrations operating at equivalent experimental conditions, and being clearly detectable for talc concentrations of 0.5%. This promoting effect of talc was more effective at higher cooling rates conditions, that is when higher amounts of least stable polymorphic forms of CB, such as Forms I and II, where crystallized. Talc also caused a meaningful increase of the onset crystallization temperature at all experimental circumstances and they exhibited logarithmic growth type, so that most important variations were detected at talc concentrations lower than 1%. The parallel arrangement of lamellar planes in layers, determined by SR-μ-XRD, confirmed that TAG molecules may be adsorbed with the long axis parallel to the normal cleavage surfaces of talc. This was determined at the lowest concentrations of 0.1% talc.

Combined effects of external factors, such as the application of dynamic thermal treatments and the addition of minor components, may permit to modulate crystallization and polymorphic

behavior of lipid systems to achieve expected physical properties by selecting appropriate conditions.

ASSOCIATED CONTENT

Supporting Information

Figure S1. Lateral enlarged view of SR-SAXD (a) and SR-WAXD (b) patterns of bulk CB when heated at 0.5 °C/min after cooled at 15 °C/min. Unit: nm.

Figure S2. Lateral view of SR-WAXD profiles in Figures 2b-d. a) Bulk CB, b) CB + 0.5% talc, and c) CB + 1% talc. Unit: nm.

AUTHOR INFORMATION

Corresponding Author

Phone: +34 93 402 13 50. Fax: +34 93 402 13 40. E-mail: laurabayes@ub.edu

Present Addresses

†Present address of the author Chinami Ishibashi is the following:

Faculty of Human Culture and Science, Prefectural University of Hiroshima, Hiroshima, Japan.

Funding Sources

Ministerio de Ciencia e Innovación; Agencia Estatal de Investigación: Grant PID2019-107032RB-I00.

ALBA synchrotron facility: Proposals 2014070991 and 2015021206.

SPring-8 synchrotron facility: Proposal 2015B1928.

ACKNOWLEDGMENT

The authors acknowledge the financial support of Grant PID2019-107032RB-I00 funded by MCIN/AEI/10.13039/501100011033/. Fundings from the ALBA and SPring-8 facilities are gratefully acknowledged. SR-XRD experiments were performed with the approval of the ALBA Scientific Advisory Committee (proposals 2014070991 and 2015021206). The authors thank Dr. Marc Malfois, responsible for the BL11-NCD-SWEET at ALBA, for his help. SR-μ-XRD experiments, carried out at SPring-8, were conducted thanks to the approval of proposal 2015B1928. Authors would like to express their gratitude to Dr. Masugu Sato, beamline scientist of beamline 46XU, and Dr. Norimichi Sano, associate chief scientist of Industrial Application Division at SPring-8.

REFERENCES

1. Cocoa Butter and Related Compounds; Garti, N., Widlak, N. R., Eds. AOCS Press: Urbana, IL, 2012.

2. Beckett's Industrial Chocolate Manufacture and Use; Beckett, S., Fowler, M. S., Ziegler, G. R., Eds.; Wiley Blackwell: Oxford, U.K., 2017.

3. Loisel, C.; Keller, G.; Lecq, G.; Bourgaux, C.; Ollivon, M. Phase Transitions and Polymorphism of Cocoa Butter. *J. Am. Oil Chem. Soc.* **1998**, 75, 425-439.

4. Van Malssen, K.; van Langevelde, A.; Peschar, R.; Schenk, H. Phase Behavior and Extended Phase Scheme of Static Cocoa Butter Investigated with Real-Time X-Ray Powder Diffraction. *J. Am. Oil Chem. Soc.* **1999**, 76, 669-676.

5. Bayés-García, L.; Calvet, T.; Cuevas-Diarte, M.A.; Rovira, E.; Ueno, S.; Sato, K. New Textures of Chocolate Are Formed by Polymorphic Crystallization and Template Effects: Velvet Chocolate. *Cryst. Growth Des.* **2015**, 15, 4045-4054.

6. Bayés-García, L.; Aguilar-Jiménez, M.; Calvet, T.; Koyano, T.; Sato, K. Crystallization and Melting Behavior of Cocoa Butter in Lipid Bodies of Fresh Cacao Beans. *Cryst. Growth Des.* **2019**, 19, 4127-4137.

7. Loisel, C.; Lecq, G.; Keller, G.; Ollivon, M. Dynamic Crystallization of Dark Chocolate as Effected by Temperature and Lipid Additives. *J. Food Sci.* **1998**, 63, 73-79.

8. Aronhime, J. S.; Sarig, S.; Garti, N. Reconsideration of polymorphic transformations in cocoa butter using the DSC. *J. Am. Oil Chem. Soc.* **1988**, 65, 1140-1143.

9. Chen, J.; Ghazani, S. M.; Stobbs, J. A.; Marangoni, A. G. Tempering of cocoa butter and chocolate using minor lipidic components. *Nat. Commun.* **2021**, 12, 5018.

10. Garti, N.; Schlichter, J.; Sarig, S. Effect of food emulsifiers on polymorphic transitions of cocoa butter. *J. Am Oil Chem. Soc.* **1986**, 63, 230-236.

11. Nakae, T.; Kometani, T.; Nishimura, T.; Takii, H.; Okada, S. Preparation of Glyceroglycolipids from Pumpkin and Their Effects on Polymorphic Transformation of Cocoa Butter. *Food Sci. Technol. Res.* **2000**, 6, 263-268.

12. Nakae, T.; Kometani, T.; Nishimura, T.; Takii, H.; Okada, S. Effect of Glycolipid Fraction on Fat Bloom in Dark and Milk Chocolates. *Food Sci. Technol. Res.* **2000**, 6, 269-274.

13. Nakae, T.; Kometani, T.; Nishimura, T.; Takii, H.; Okada, S. Effects of Glyceroglycolipids Prepared from Various Natural Materials on Polymorphic Transformation of Cocoa Butter. *Food Sci. Technol. Res.* **2000**, 6, 320-323.

14. Tietz, R.A.; Hartel, R.W. Effects of Minor Lipids on Crystallization of Milk Fat-Cocoa Butter Blends and Bloom Formation in Chocolate. *J. Am. Oil Chem. Soc.* **2000**, 77, 763-771.

15. Walter, P.; Cornillon, P. Influence of Thermal Conditions and Presence of Additives on Fat Bloom in Chocolate. *J. Am. Oil Chem. Soc.* **2001**, 78, 927-932.

16. Jovanovic, O.; Pajin, B. Influence of lactic acid ester on chocolate quality. *Trends Food Sci. Technol.* **2004**, 128-136.

17. Pajin, B.; Jovanovic, O. Influence of high-melting milk fat fraction on quality and fat bloom stability of chocolate. *Eur. Food Res. Technol.* **2005**, 220, 389-394.

18. Smith, K.W.; Bhaggan, K.; Talbot, G.; van Malssen, K.F. Crystallization of Fats: Influence of Minor Components and Additives. *J. Am. Oil Chem. Soc.* **2011**, 88, 1085-1101.

19. Mahisanunt, B.; Hondoh, H.; Ueno, S. Coconut Oil Crystallization on Tripalmitin and Tristearin Seed Crystals with Different Polymorphs. *Cryst. Growth Des.* **2020**, 20, 4980-4990.

20. Yoshikawa, S.; Kida, H.; Sato, K. Promotional Effects of New Types of Additives on Fat Crystallization. *J. Oleo Sci.* **2014**, 63, 333-345.

21. Yoshikawa, S.; Kida, H.; Sato, K. Fat crystallization with talc particles is influenced by particle size, concentration, and cooling rate. *Eur. J. Lipid Sci. Technol.* **2015**, 117, 858-868.

22. Yoshikawa, S.; Kida, H.; Sato, K. Adding talc particles improves physical properties of palm-oil-based shortening. *Eur. J. Lipid Sci. Technol.* **2016**, 118, 1007-1017.

23. Kaneko, F.; Yamamoto, Y.; Yoshikawa, S. Structural Study on Fat Crystallization Process Heterogeneously Induced by Graphite Surfaces. *Molecules* **2020**, 25, 4786.

24. Ueno, S.; Nishida, T.; Sato, K. Synchrotron Radiation Microbeam X-ray Analysis of Microstructures and the Polymorphic Transformation of Spherulite Crystals of Trilaurin. *Cryst. Growth Des.* **2008**, 8, 751-754.

25. Bayés-García, L.; Calvet, T.; Cuevas-Diarte, M.A.; Ueno, S.; Sato, K. Heterogeneous microstructures of spherulites of lipid mixtures characterized with synchrotron radiation microbeam X-ray diffraction. *CrystEngComm* **2011**, 13, 6694-6705.

26. Verstringe, S.; Dewettinck, K.; Ueno, S.; Sato, K. Triacylglycerol Crystal Growth: Templating Effects of Partial Glycerols Studied with Synchrotron Radiation Microbeam X-ray Diffraction. *Cryst. Growth Des.* **2014**, 14, 5219-5226.

27. Shinohara, Y.; Takamizawa, T.; Ueno, S.; Sato, K.; Kobayashi, I.; Nakajima, M.; Amemiya. Microbeam X-ray Diffraction Analysis of Interfacial Heterogeneous Nucleation of n-Hexadecane inside Oil-in-Water Emulsion Droplets. *Cryst. Growth Des.* **2008**, 8, 3123-3126.

28. Arima, S.; Ueno, S.; Ogawa, A.; Sato, K. Scanning Microbeam Small-Angle X-ray Diffraction Study of Interfacial Heterogeneous Crystallization of Fat Crystals in Oil-in-Water Emulsion Droplets. *Langmuir* **2009**, 25, 9777-9784.

29. Wassell, P.; Okamura, A.; Young, N.W.G.; Bonwick, G.; Smith, C.; Sato, K.; Ueno, S. Synchrotron Radiation Macrobeam and Microbeam X-ray Diffraction Studies of Interfacial Crystallization of Fats in Water-in-Oil Emulsions. *Langmuir* **2012**, 28, 5539-5547.

30. Tanaka, L.; Tanaka, K.; Yamato, S.; Ueno, S.; Sato, K. Microbeam X-ray Diffraction Study of Granular Crystals Formed in Water-in-Oil Emulsion. *Food Biophysics* **2009**, 4, 331-339.

31. PerkinElmer. Instructions Model DSC-4; Norwalk, Connecticut, USA, 1982.

32. Kieffer, J.; Karkoulis, D. PyFAI, a versatile library for azimuthal regrouping. *J. Phys. Conf. Ser.* **2013**, 425, 202012.

33. Mykhaylyk, O.O.; Smith, K.W.; Martin, C.M.; Ryan, A.J. Structural models of metastable phases occurring during the crystallization process of saturated/unsaturated triacylglycerols. *J. Appl. Cryst.* **2007**, 40, s297–s302.

34. Bayés-García, L.; Calvet, T.; Cuevas-Diarte, M.A.; Ueno, S.; Sato, K. In situ synchrotron radiation X-ray diffraction study of crystallization kinetics of polymorphs of 1,3-dioleoyl-2-palmitoyl glicerol (OPO). *CrystEngComm.* **2011**, 13, 3592-3599.

35. Bayés-García, L.; Calvet, T.; Cuevas-Diarte, M.A.; Ueno, S.; Sato, K. In situ observation of transformation pathways of polymorphic forms of 1,3-dipalmitoyl-2-oleoyl glycerol (POP) examined with synchrotron radiation X-ray diffraction and DSC. *CrystEngComm*. **2013**, 15, 302-314.

36. Bayés-García, L.; Calvet, T.; Cuevas-Diarte, M.A.; Ueno, S.; Sato, K. Crystallization and Transformation of Polymorphic Forms of Trioleoyl Glycerol and 1,2-Dioleoyl-3-rac-linoleoyl Glycerol. *J. Phys. Chem. B* **2013**, 117, 9170-9181.

37. Bayés-García, L.; Calvet. T.; Cuevas-Diarte, M.A.; Ueno, S. In situ crystallization and transformation kinetics of polymorphic forms of saturated-unsaturated-unsaturated triacylglycerols: 1-palmitoyl-2,3-dioleoyl glycerol, 1-stearoyl-2,3-dioleoyl glycerol, and 1-palmitoyl-2-oleoyl-3-linoleoyl glycerol. *Food Res. Int.* **2016**, 85, 244-258.

FOR TABLE OF CONTENTS USE ONLY

Heterogeneous nucleation effects of talc particles on polymorphic crystallization of cocoa butter

Laura Bayés-García[a], Shinichi Yoshikawa[b], Mercedes Aguilar-Jiménez[a], Chinami Ishibashi[c,†], Satoru Ueno[c], Teresa Calvet[a]

[a]Departament de Mineralogia, Petrologia i Geologia Aplicada, Facultat de Ciències de la Terra, Universitat de Barcelona, Martí i Franquès, s/n, 08028, Barcelona, Spain

[b]Research Institute for Creating the Future, Fuji Oil Holdings INC., Osaka, Japan.

[c]Faculty of Applied Biological Science, Hiroshima University, Higashi-Hiroshima, Japan.

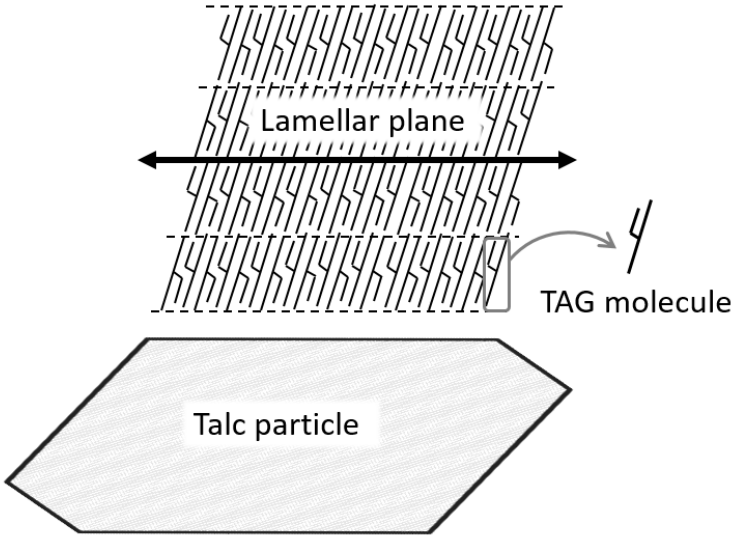

We studied the heterogeneous nucleation effects caused by talc nanoparticles when added to cocoa butter. Talc caused a significant increase of the onset crystallization temperatures and also acted as polymorphic stabilizer. The determination of lamellar plane directions of triacylglycerol molecules oriented with talc addition permitted to define a tentative model on their arrangement on talc particles surface.